A Fusion Approach for Tree Crown Delineation from Lidar Data

Colin J. Gleason and Jungho Im

Abstract

This study proposes a multi-step method (the COTH method) to delineate individual tree crowns in dense forest conditions using lidar data, with the intent for the final delineation results to be used in a biomass estimation study. The study was conducted for an even-aged Norway Spruce (Picea abies) plantation containing 188 trees located in Tully, New York, and owned by the State University of New York College of Environmental Science and Forestry (SUNY ESF). Lidar data with a point density of 12.7 points/m^2 was collected in August 2010, and field data were collected to measure tree height and species in August 2010 as well. Field data containing tree height and crown width, an important component of treetop detection, were collected in summer 2006. By combining heuristically (genetic algorithm) optimized object recognition to detect tree crown objects, local maxima filtering with variable window size to detect treetops, and a modified hill climbing algorithm to segment crown objects; treetops were identified with 86.2 percent accuracy and 23.9 percent commission error. The overall areal accuracy of the delineation was 72.5 percent. The automated COTH method represents an improvement in crown delineation accuracy for lidar data.

Introduction

Increased understanding about the importance of forests as carbon sequestration centers and potential feedstock for biofuel production has lead to numerous studies attempting to quantify and characterize forests in accurate detail (Gleason and Im, 2011a). While field-based methods have long been used by professional foresters to understand the dynamics of the forest, these methods are often difficult to implement over large land areas or in rugged terrain. Of principal interest in quantifying forests is accurately modeling forest biomass, which provides critical input for estimates of carbon sequestration, total carbon, and biofuel potential. Remotely sensed data provides an outlet for biomass estimation that can be quickly and safely attained, and methods to quantify biomass from such data are a widely studied branch of forest investigation (Gonzalez *et al.*, 2010; Koch, 2010). A summary of recent research efforts to estimate biomass from remotely sensed data can be found in Gleason and Im (2011a). A subset of these remote sensing studies focuses on aggregating the biomass of each tree in a forested plot to form an estimate of the biomass of the plot as a whole, and these methods have proved effective so long as the number and dimensions of the trees are accurately identified (Naesset and Okland, 2002; Popescu and Wynne, 2004; Bortolot and Wynne, 2005; Chen *et al.*, 2007; Popescu, 2007; Gonzalez *et al.,* 2010, Kwak *et al.,* 2010). Optical sensors with resolution less than 2 m or airborne lidar data are ideal for such analysis, as their fine spatial resolution allows more precise tree crown delineation (Naesset and Okland, 2002). Optical data employed for such studies may include high resolution satellite imagery (e.g., QuickBird, Ikonos) as well as more traditional aerial photography. While biomass estimation studies commonly use coarser resolution satellite data (e.g., Landsat, SRTM), such scales are unsuitable for determining the boundaries of individual trees.

Early research investigating individual tree delineation associated remotely sensed data with tree crowns identified in the field (Naesset and Okland, 2002). Research advanced when trees were automatically detected, most often accomplished through the process of local maxima filtering of various remotely sensed data such as optical and lidar data (Wulder *et al.*, 2000; Persson *et al.,* 2002; Popescu and Wynne, 2004; Bunting and Lucas, 2006; Jang *et al.* 2008; Zhao *et al.,* 2009). Local maxima filtering operates with the assumption that tree tops are represented by local maxima within a crown. When applied to lidar data, these treetops can be assigned a height, and biomass can be calculated based on regression and species allometry (Popescu and Wynne, 2004). As local maxima in a fixed search window often return many spurious treetops, maxima transformations and variable search windows are necessary to reduce these commission errors (Chen *et al.,* 2006; Kwak *et al.,* 2007). Another method of defining treetops is template matching, in which the remotely sensed representations of known treetops from field data are passed over an image/lidar surface and those pixels with the highest correlation are considered treetops (Ke *et al.,* 2010; Vauhkonen *et al.,* 2010).

Once treetops have been identified, the next logical step is to define the crowns for each of these treetops. Planimetrically, a tree crown is a roughly circular polygon when viewed from the nadir direction, and crown width is highly correlated to diameter at breast height (DBH), which is needed for allometric equations to estimate biomass (Popescu, 2007). A tree crown is an irregular volume determined by the physical characteristics of the site in which it is found, and is much more complex than a planimetric footprint would suggest. To recreate such a shape requires treetop location and height data within the tree crown footprint to create a surface, sometimes called a crown geometric volume (Brandtberg, 2007; Kato *et al.,* 2009; Breidenbach *et al.,* 2010; Kwak *et al.,* 2010).

Colin J. Gleason and Jungho Im are with the Department of Environmental Resources Engineering, State University of New York, College of Environmental Science and Forestry, One Forestry Dr., Syracuse, NY 13210 (imj@esf.edu).

Photogrammetric Engineering & Remote Sensing
Vol. 78, No. 7, July 2012, pp. 000–000.

0099-1112/12/7807–0000/$3.00/0

To define a tree crown in two dimensions, watershed processing is commonly used with both imagery and lidar data, which treats each treetop as a basin that captures water (Wang *et al.,* 2004; Chen *et al.,* 2006; Chen *et al.,* 2007; Kwak *et al,* 2007; Castilla *et al.,* 2008; Kato *et al.,* 2009; Kwak *et al.,* 2010). Alternatively, object recognition algorithms using a crown-following approach or image segmentation have proved successful in delineating trees for both optical images and lidar data (Gougeon, 1995; Bunting and Lucas, 2006; Coops *et al.,* 2008; Jang *et al.,* 2008; van Aardt *et al.,* 2008; Chen *et al.,* 2010; Ke *et al.,* 2010). Object recognition has shown great promise in tree crown segmentation when used in conjunction with imagery, and has only recently been adopted for use with lidar data (Ke *et al.*, 2010; Lin *et al.*, 2011).

Lidar data has become widely used for forest research, and more specifically high-density airborne lidar data is used because of its ability to accurately depict tree height, crowns, and canopies (Gleason and Im, 2011a). Lidar has an advantage over optical imagery for biomass estimation for this reason, and Coops *et al.* (2008) found that lidar was better suited to crown identification than aerial imagery. This may not always be the case, as segmentation processes are strongly influenced by shadowing, look angle, and relative relief of forest structure, yet with biomass estimation intended as a final product for most segmentation studies, lidar remains a premier sensor option (Gleason and Im, 2011a).

Our goal is to develop an automated and robust method for determining individual trees from discrete multiple-return airborne lidar data so that the method can be used in a biomass or carbon stock estimation study. Our research combines heuristic optimization of an object classification algorithm originally intended for medical imagery (Li *et al.,* 2007) in conjunction with established methods of treetop detection. The method has been named Crown delineation based on Optimized object recognition, Treetop identification, and Hill-climbing (COTH). Heuristic optimization is important because many object recognition algorithms contain a large number of parameters that severely impact the results of the segmentation, and are also computationally expensive. As the results of segmentation are critically important to any estimates of biomass, it is important that the process be performed as accurately as possible (van Aardt *et al.,* 2008). We used a heuristic optimization approach (specifically a genetic algorithm (GA)) to allow for an accurate solution to be found much more quickly than by exhaustive search or by accepting default parameters. GAs have been used to model forest parameters successfully before, and have been shown to be an effective and easily understood method for parameter optimization (Fang *et al.,* 2003; Rezende *et al.,* 2008; Tseng *et al,* 2008; Gong *et al.*, 2011). Given that biomass estimation is a hot research topic in recent years (Gleason and Im, 2011a), algorithm improvements are necessary to achieve higher accuracies of biomass estimation while increasing the automation of the process, allowing for greater transferability and power of biomass estimation methods. Comparison is given between watershed processing and the COTH method to illustrate the difference in results between the two.

Study Area and Data

Study Area

This study was conducted for an area of Heiberg Memorial Forest, located in Tully, New York, containing an even-aged Norway spruce (*Picea abies*) plantation planted in 1931 (Figure 1). State University of New York College of Environmental Science and Forestry (SUNY ESF) has owned and managed the plantation since its inception in 1931.The forest was thinned in 1980 and the original spacing of the plantation was in a 2 m grid.

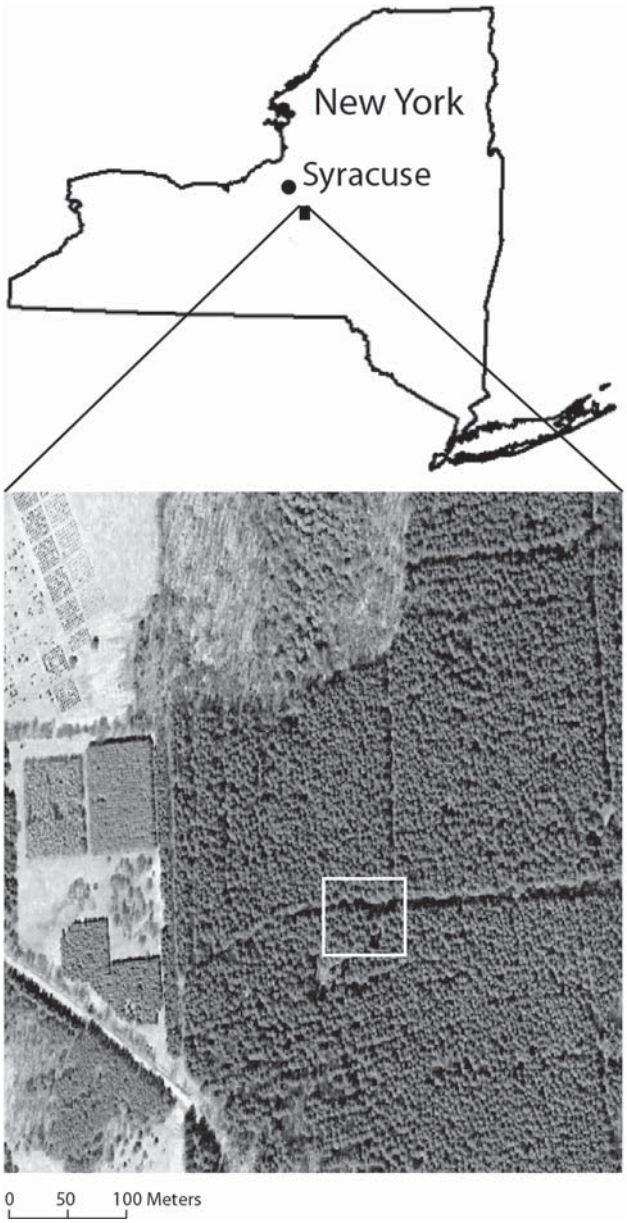

Figure 1. The study site (white rectangle) within Heiberg Forest, Tully, New York. (2006 aerial orthophoto, New York State GIS Clearinghouse (*http://www.nysgis.state.ny.us/*).

Lidar Data

The discrete multiple-return lidar data for this study was acquired on 10 August 2010, using an airborne ALS60 sensor by the Kucera International Inc. (Table 1). Raw laser data was post-processed by the vendor using the TerraSolid software suite and manual editing, and resulted in creation of a canopy point cloud. The object recognition method used in this study requires a data raster, and thus a canopy surface raster (i.e., DSM) was created from the canopy point cloud (i.e., first return) using inverse distance weighted

TABLE 1. CHARACTERISTICS OF THE LIDAR DATA COLLECTION ON 10 AUGUST 2010

Pulse rate	183.8 khz
Field of View	28 degrees
Altitude	487 m
Flying Speed	150 knots
Point Density	>7 pts/m^2

(IDW) interpolation in ArcGIS® 9.3. This is a valid method of surface creation for this study because of the high point density of the lidar data, which decreases the likelihood of interpolation error and eliminates the need for more sophisticated surface creation (Popescu *et al.,* 2002). A canopy height raster was created by subtracting the last return-based bare earth elevation from canopy surface raster, leaving an image where each pixel corresponds to the uppermost elevation recorded for that location by the lidar sensor. Such a raster surface can be used in place of optical imagery for object recognition, and is shown in Figure 2.

Reference Data

Reference data for this study were initially generated by manually interpreting 2006 aerial orthophotos (Ke *et al.*, 2010). The natural color orthophotos for this site were provided by the New York State GIS Clearinghouse (*http://www.nysgis.state.ny.us/*), and have a shallow look angle in the portion of the frame that corresponds to our study site and 0.6 m spatial resolution. Three interpreters manually delineated crowns as polygons from these 2006 orthophotos using ArcGIS® 9.2, and a total of 239 reference crowns were identified, with an average crown area of 11.4 m^2. Growth and mortality occurred in the forested plot between the 2006 aerial imagery and the 2010 collection of lidar data, so the crown reference map was updated accordingly. Starting with the 2006 crown map, crown polygons were either reshaped or deleted, depending on the presence of the trees within a contrast enhanced lidar-derived surface. The overall change in area of the tree crown polygons was 6.1 percent, and the new map contains 188 tree crowns with an average area of 13.2 m^2.

In August of 2010, field crews measured specific tree heights to verify the accuracy of the lidar data covering continuous forest inventory plots maintained by SUNY ESF. These plots are inventoried every 10 years, and are located using differential GPS positioning with sub-meter precision. While these inventory plots were able to verify the accuracy of the lidar data, there were not enough of such plots inside the study area to be used as ground reference trees. Therefore, only the updated crown map was used as reference data for accuracy assessment.

Methods

The COTH method used to delineate tree crowns in this study is a synthesis of three methods: treetop identification, optimized object recognition, and modified hill climbing to associate crowns with treetops (Figure 3). First, an object recognition algorithm was modified and applied to identify tree crowns and tree crown clusters. Recently, Lin *et al.* (2011) used an active contouring algorithm for object recognition, and reported 69 percent to 81 percent detection accuracy for three species, which correspond to treetop identification accuracy. In a similar study, Ke *et al.* (2010) used an active contouring algorithm based on local binary fitting energy (Li *et al.,* 2007) to identify crown objects using aerial photographs of coniferous trees, resulting in good performance (65 percent to 85 percent areal agreement with reference crowns). The contouring method of Li *et al.* (2007), originally developed for medical images, was based on level set theory (Chan and Vese, 2001), and used local binary fitting energy to drive an active contouring process resulting in objects of either crowns or crown clusters. A level set method sets a value of 0 on an initial contour, with a negative constant value inside the contour and a positive constant value outside. This contour then evolves as a

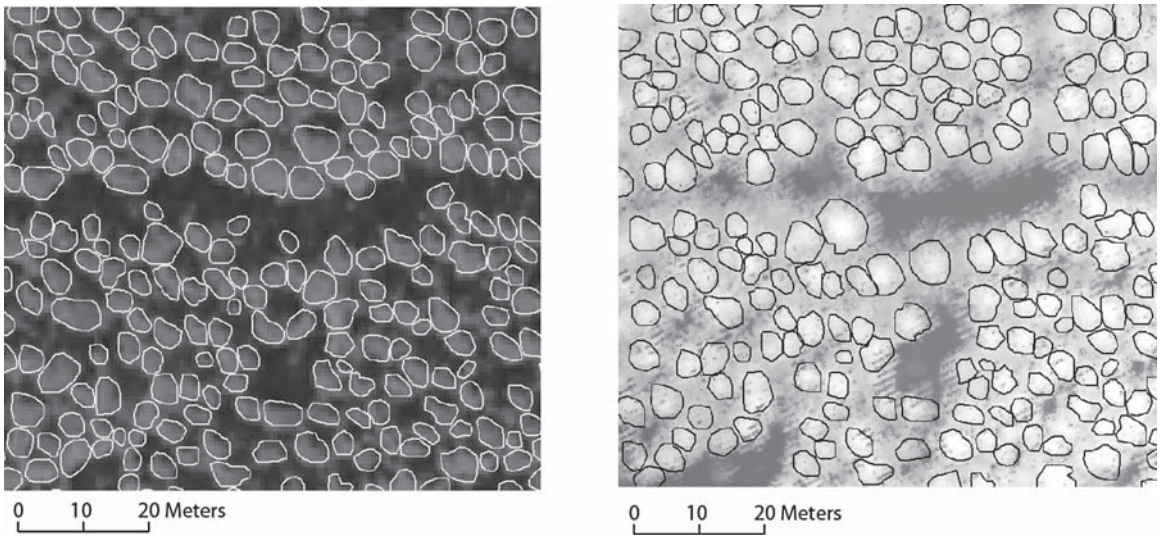

Figure 2. (a) 2006 natural color orthoimagery and manually delineated reference crowns, and (b) the updated reference map and the lidar-derived canopy height surface.

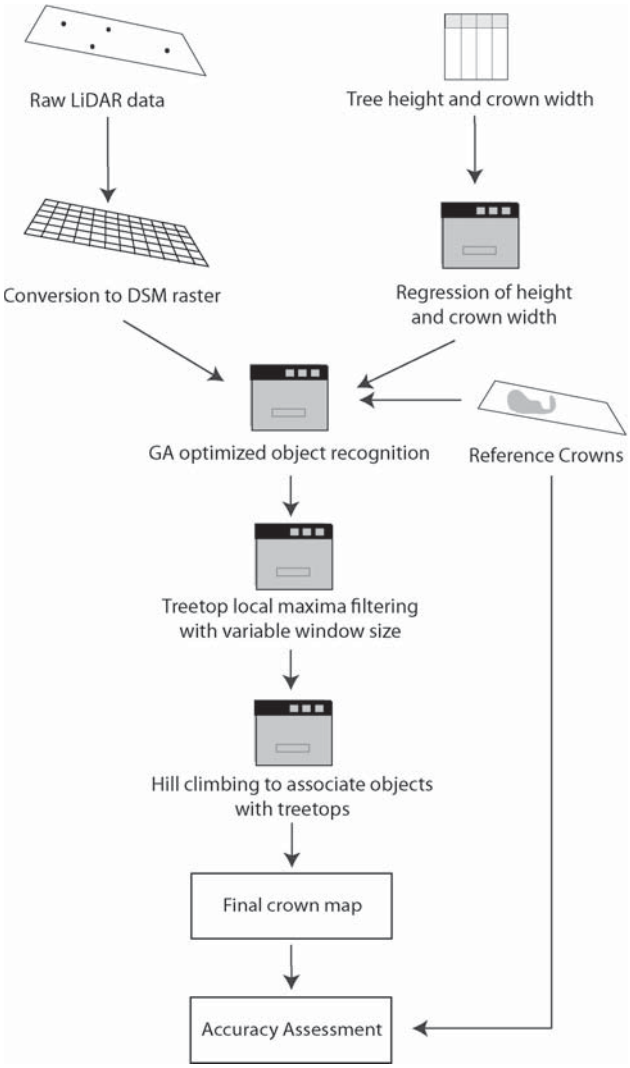

Figure 3. Process flow diagram of the COTH method.

function of the input image and its relation to the contour. The energy function used in this study is:

$$Ex = \lambda_1 \int_{in(C)}^{\mu} k(x-y)|I(y)-f_1(x)|_2 dy + \lambda_2 \int_{out(C)}^{\nu} k(x|y)|I(y)|f_2(x)|_2 dy \quad (1)$$

where E is the image energy that will be minimized, and λ_1 and λ_2 represent interior and exterior energy constants that regulate contour directional movement; I is the image, and G represents the contour in the image; f_1 and f_2 are weighted values that localize the contour near the point x; and μ and υ interact with these terms to assure a stable evolution of the contour (Adapted from Li *et al.,* 2007).

There are five parameters that affect the results of the clustering, and misconfiguring these parameters could result in over-segmentation, under-segmentation, or simply one large object (Table 2). Adjusting these parameters to achieve robust clustering results is computationally expensive, as each run of the method requires considerable processing time when applied to lidar data. The method also requires an initial contour, and deviation of this contour from objects in the image results in increased processing time. To mitigate this, we set the initial contour equal to the boundaries of the segments identified using watershed processing following the method of Chen *et al.* (2006). This greatly reduced the processing time of the clustering algorithm, but still required manual manipulation of the object recognition parameters. To efficiently optimize the clustering parameters, we took advantage of the speed and flexibility of a heuristic GA.

Table 2. Five Key Parameters Used in the Object Recognition Algorithm (refer to Ke et al., 2010; Li et al., 2007)

Parameter	Effect
λ_1	Interior energy constant, with λ_2, controls expansion/contraction rate of contours
λ_2	Exterior energy constant
μ	Stability constant, controls speed of contraction/expansion
υ	Level curve length constant, regulates overall size of contours
Iterations	Number of iterations

Genetic Algorithms

GAs mimic the natural processes of natural selection and evolution, and simulate these processes on a set of potential solutions to a problem. These potential solutions are called chromosomes, typically consisting of a set of parameters (i.e., genes) required to implement a particular process (Chang *et al.,* 2009). A fitness function evaluates the ability of a particular chromosome to survive and is usually based on an accuracy or robustness measure intrinsic to the optimization problem at hand, thus requiring little additional mathematical knowledge and making GAs applicable for a wider range of problems over other mathematical optimization methods (Wang, 2005). For this study, a fitness function was determined by measuring the total area of the reference crowns and comparing this area to the area covered by the crown clusters from the object recognition algorithm. Therefore, the GA seeks to match the area of produced crowns to the area of reference crowns as closely as possible. Each chromosome for this GA has five genes that correspond to the five parameters that are the major drivers of the clustering algorithm.

The major drivers of a GA are the processes of selection, crossover, and mutation (Goldberg, 1989). The chromosome with the highest fitness level is exempt from the processes of mutation and crossover, and other chromosomes with high fitness are more likely to continue to the next generation (i.e., selected). Crossover and mutation are not guaranteed for each chromosome, and are here controlled by random processes that depend on a crossover and mutation rate. A high crossover rate mimics sexual reproduction, while a low crossover rate simulates asexual reproduction, where genes are not shared among chromosomes. For this study, we chose a crossover rate of 80 percent, which should produce a more efficient solution and is consistent with other analysis of remotely sensed data using GAs (Im *et al.*, 2011). If a chosen chromosome has been selected for crossover, it will switch certain genes with certain other chromosomes, as defined by the rules set at the beginning of the algorithm. For this study, we adopted a similar set of chromosome crossover rules as Im *et al.* (2011), where a gene chosen at random switches between predefined sets of genes and chromosomes based on their fitness ranking (Figure 4). Unlike the high crossover rate, we chose a low mutation rate of 20 percent, which mimics the somewhat rare process of natural mutation but still allows for the random altering of specific genes. In a mutation, certain genes are replaced by either a random value or a percentage

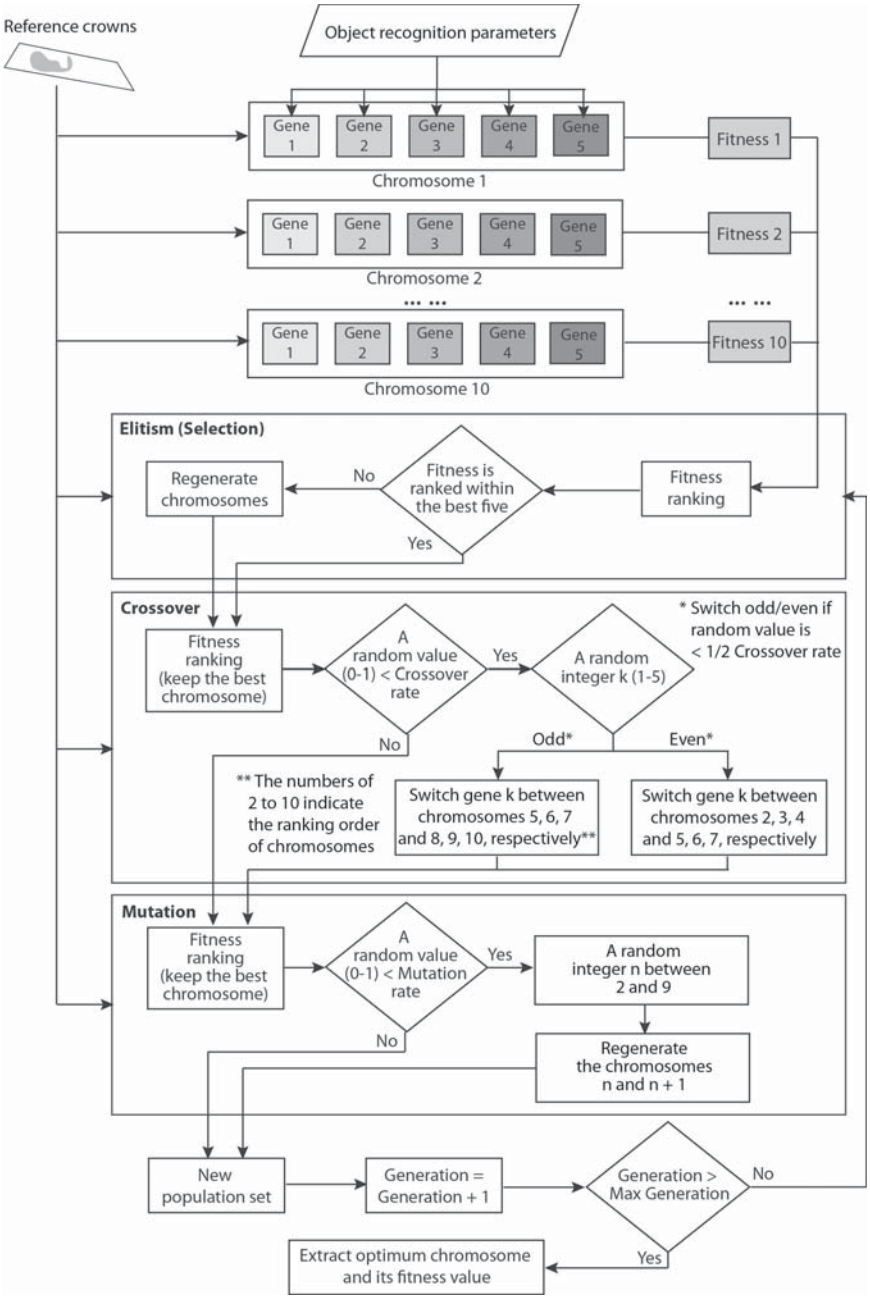

Figure 4. Flow diagram of GA developed in this study. The parameters used are the crossover rate = 0.8, mutation rate = 0.2, and number of generations = 10. Genes 1 and 2 correspond to λ_1 and λ_2, respectively, while genes 3, 4, and 5 represent μ, υ, and the number of iterations for the clustering algorithm. For the final result, μ and υ were constrained to equal 1.

change of their previous value. As before, the chromosome with the highest fitness is exempt from this process, ensuring that the best set of parameters from the previous generation is allowed to remain as a solution until it has been bettered. The number of generations for which these chromosomes undergo these processes can be predefined or based on reaching a threshold of fitness. For our study, we chose a static number of 10 generations as a maximum, due to the lengthy processing required and the similar accuracy of the solutions attained after these generations.

Treetop Detection

Once the object recognition algorithm was optimized and tree crown objects were identified, the next step was to identify treetops so crown objects could be associated with their corresponding trees. To identify these treetops, we used the method of Chen *et al.* (2006), as this provided more accurate results than fixed window local maxima filtering by incorporating field data to modify the size of the search window. Chen *et al.* (2006) proposed using the lower limit of the prediction interval obtained from regression of tree

height and crown width as measured in the field to define the search radius for local maxima. This should yield better treetop detection because in areas of lower lidar height, the trees should be smaller, and thus a smaller search window should identify more local maxima than one designed for large trees. In addition, in the tallest sections of the study site, the trees are much larger; in these locations, a large search radius will reduce the appearance of spurious local maxima. The field data necessary to define this relationship were collected in 2006 for our study site, and contain the distance to the edge of the crown from the bole for each of the four cardinal directions for every tree in the study area. This method could lead to commission error if the prediction interval is too wide; therefore Chen *et al.* (2006) proposed that larger values of (statistical confidence level) should be used to limit the width of the prediction interval. For this study, an of 0.1 was used, which is consistent with Chen *et al.* (2006). An iterative adjustment of the from 0.01 to 0.5 produced little change in the treetop detection results.

Hill Climbing

Finally, with crown objects and treetops identified, the hill climbing method proposed in Ke *et al.* (2010) was used to separate crown clusters into individual crowns and to eliminate false objects. While their method was successfully implemented for optical sensor data, it had not been tested for lidar-generated surfaces prior to the current research. Their method uses a hill climbing method to associate each pixel within a crown object to its corresponding treetop. For each pixel within a crown object, a set of movement rules is defined: (a) a *bug* is set at the starting pixel; (b) the bug moves to the 8-neighbor (adjacent raster pixels) with the greatest increase in elevation; and (c) this process is repeated until the bug reaches a predefined treetop, in which case the original bug pixel is labeled as belonging to that treetop. If the bug cannot climb to any pixel and it is not at a treetop, then logically it has reached a local maximum. To avoid these, the bug is allowed to decrease in elevation provided such a decrease is below a set threshold. If no such avenues exist, the starting pixel for the bug is labeled as not belonging to a treetop, and is eliminated from the crown map. Otherwise, the bug can continue its journey until it reaches a treetop that falls within the same crown cluster it began in. Performing this hill-climbing step eliminates all clusters that do not have a treetop in them, making the accuracy of the treetop detection paramount. This method also allows for a wide variety of crown geometries to be associated with a treetop, something template matching and shape matching cannot replicate. Computationally, the exhaustive nature of the hill climbing makes for a lengthy process, but because hill climbing is only implemented within identified crown objects, processing time is kept to a manageable level (<12 hours). The threshold used to define the ability of the hill-climbing method to decrease in height was set at 0.3 m, which allows the hill climbing to overcome any valleys within the canopy surface. The threshold also ensures that almost all crown area defined by the object recognition will be included in the final crown map and not rejected by the hill climbing. Once this portion of the COTH method is complete, the results are a final map showing the tree crown footprints for each treetop captured by the lidar data. Figure 5 presents a simple illustration of how the hill climbing method operates.

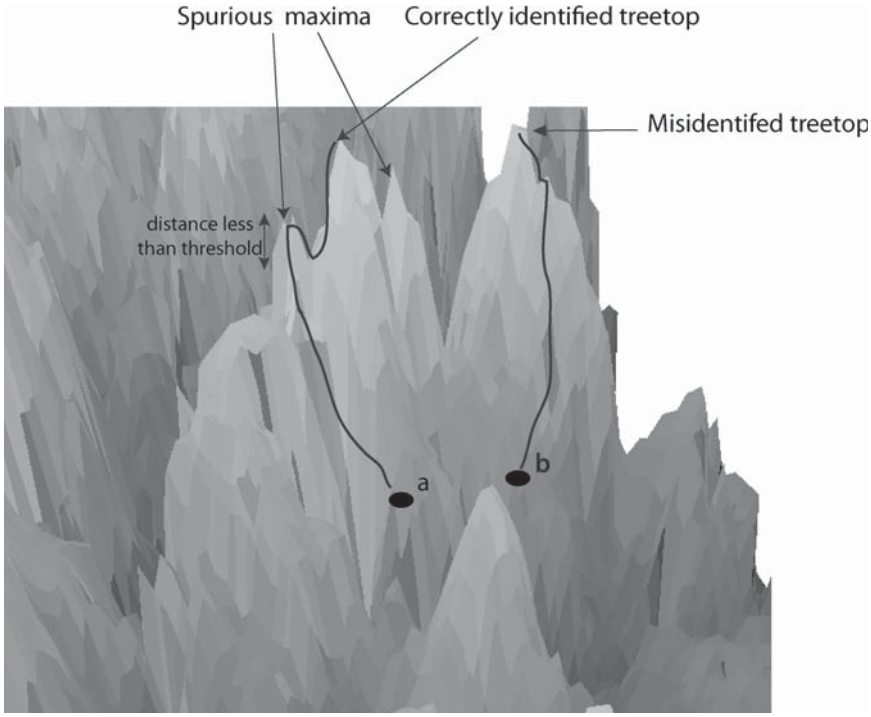

Figure 5. Two scenarios for the hill climbing portion of the method. In starting position 'a' the *bug* climbs to a spurious maxima, moves downhill within the threshold, and then continues to find a treetop. This process would associate point 'a' with the treetop at the end of its trail. Starting at point 'b' the bug climbs to a treetop that was not identified in the previous step. The bug cannot move down from the treetop, is trapped, and point 'b' is not associated with any crown: an error with the treetop identification step.

Accuracy Assessment

Accuracy assessment for tree crown delineation should contain several features. First, a measure of how many trees in the study site were correctly identified with a unique delineated crown should be given. In some cases, a cluster of trees with small DBH will appear as one crown in a forest canopy, and in this case the uniqueness of tree crown-field tree may be ignored and the delineation considered accurate (Bunting and Lucas, 2006). This step assumes that the study has accurate field data that correctly identify the location of each tree in the study plot, and if not, the number of treetops identified by the treetop identification step was checked against the reference crowns map delineated from imagery. Second, a measure of crown area, which is highly correlated to biomass, should be included (Popescu, 2007). Chen *et al.* (2006) proposed that a crown has areal accuracy when there is one delineated crown that is spatially coincident (overlapping) with a single reference crown, and the area of the delineated crown is within 10 percent of the reference crown area. Such crowns define a "1 to1 relationship," and the area of these crowns divided by total reference crown area is referred to as absolute accuracy for tree isolation (AATI) (Chen *et al.*, 2006). Kwak *et al.* (2007) and Kwak *et al.* (2010) used a similar metric to determine crown area: in their metric, delineated crowns were classified as either correct (one-to-one correspondence) or satisfactory (areal similarity based on overlap). Other methods of accuracy assessment include a total area comparison, in which the total area of reference crowns are compared with the total area delineated as crown, and implicit delineation assessment through biomass quantification accuracy (Wang *et al.,* 2004; Popescu, 2007; Zhao *et al.,* 2009).

For this study, we chose to include several measures of accuracy, beginning with treetop detection accuracy. Because the hill-climbing algorithm can only climb to a treetop within a crown object, if treetops are omitted the crown cluster will not be delineated. Therefore, it is essential that treetops be accurately identified. Commission error, which can be a problem with treetop detection methods (Chen *et al.*, 2006), only becomes relevant if the object recognition method locates a crown cluster around these extra treetops, so the influence of the commission error can be reduced if the object recognition is robust, which is an advantage of the COTH method. While the accuracy of the treetop detection is excellent, it still limits the areal accuracies of the clustering and hill climbing processes, which can be accounted for in the area of crowns belonging to those treetops not identified.

Second, tree crown classification accuracy is reported, showing a confusion matrix to discern the accuracy of identifying both crown and non-crown areas. This approach is included because it accounts for the areal discrepancy between reference crowns and those produced by delineation methods. Existing accuracy assessment methods that compare only the number of trees correctly delineated to those in error do not encompass the magnitude of the areal difference for those crowns incorrectly identified. This error may be significant, especially if the delineation method cannot correctly define tree crowns for dominant trees that may border a gap in the canopy and have significant influence on forest dynamics. As a comparison between these assessment methods, we report accuracy as both the aforementioned classification accuracy and the AATI statistic proposed by Chen *et al.* (2006). In addition, several tree crown-based and landscape-based metrics are calculated for reference crowns and those produced by delineation methods. The metrics used are area, perimeter, circle, and fractal at the crown level and contagion, division, split, and fractal at the landscape level (Table 3). These metrics would be meaningful for comparing the tree crown delineation methods especially for dense forest with significant gaps such as the study area.

Results

The results of this study are presented according to the accuracy metrics described in the accuracy assessment section, and four research scenarios are presented for comparison: COTH delineation, watershed delineation, and two variants of the COTH method. These additional methods are referred to as COTH-M (manually manipulating the parameters of the object recognition) and COTH-D (using the default parameters). Table 4 shows a hierarchy of these configurations used for comparison of the COTH results. COTH-D and COTH-M are presented to illustrate the increases in accuracy obtained by including the GA as part of the COTH method.

TABLE 3. TREE CROWN-BASED AND LANDSCAPE-BASED METRICS

Tree crown-based		Landscape-based	
Area	Equals crown area	Contagion	Equals 1 minus the sum of the proportional abundance of tree and non-tree multiplied by the proportion of adjacencies between cells of tree and non-tree, multiplied by the logarithm of the same quantity, summed over each type (i.e., tree and non-tree); divided by 2 times the logarithm of 2 (i.e., tree and non-tree); multiplied by 100 (to convert to a percentage).
Perimeter	Equals crown perimeter	Division	Equals 1 minus the sum of crown area (m^2) divided by total study area (m^2), quantity squared, summed across all crowns in the area. As crown area increases, it approaches to 1.
Circle	Equals 1 minus crown area (m^2) divided by the area (m^2) of the smallest circumscribing circle. 0 for circular crowns and approaches 1 for elongated.	Split	Equals the total study area (m^2) squared divided by the sum of crown area (m^2) squared, summed across all crowns in the area. It increases as the focal crown type (i.e., crown and non-crown) is increasingly reduced.
Fractal	Equals 2 times the logarithm of crown perimeter (m) divided by the logarithm of crown area (m^2). It reflects shape complexity across a range of crown sizes.	Perimeter-Area Fractal	Equals 2 divided by the slope of regression line obtained by regressing the logarithm of crown area (m^2) against the logarithm of crown perimeter (m).

Table 4. Selected Methods for Comparison of Results

Method	Description
Watershed	Watershed processing
COTH	COTH processing
COTH-m	COTH w/ manual object recognition parameters
COTH-d	COTH w/ default object recognition parameters

The COTH method was able to identify tree crowns with 72.5 percent classification accuracy, whereas using COTH-M yielded 66.0 percent accuracy (Table 5; Figure 6). This accuracy was investigated to determine the need for the object recognition step in COTH. Using the watershed delineation method produced a crown map with 43.0 percent classification accuracy (Figure 6a). Watershed delineation is severely hampered by its inability to produce non-crown area, hence the low accuracy for non-dense forest conditions. The treetop identification step correctly identified 86.2 percent of reference crowns in the study area with a unique treetop, and also contained a commission error of 23.9 percent. The final parameters used in the optimized object recognition algorithm were $\lambda_1 = 0.72$, $\lambda_2 = 1.29$, $\mu = 1.0$, $\nu = 1.0$, and 624 iterations (Figure 7).

Table 5 summarizes the confusion matrices for accuracy assessments of the four scenarios. Much attention is paid to the object recognition step in the subsequent discussion, as the accuracy of the COTH method is most strongly tied to the identification of crown objects. The treetop identification and hill climbing steps are relatively straightforward and have fixed parameters, so they are not included as different delineation scenarios. Using the GA to optimize the object recognition significantly increased the accuracy of the final delineation over using the default parameters and manually adjusting the driving parameters. When assessing accuracy using the AATI statistic proposed by Chen *et al.* (2006), the accuracy of the COTH method was 18.1 percent, yet decreasing the overlap tolerance from 90 percent to 60 percent pushes the COTH AATI to 61.3 percent. This 60 percent overlap is introduced for practical reasons, as it may represent a correctly identified crown that is shifted from

Table 5. Error Matrices of Tree Crown Delineation Using (a) the watershed delineation method, (b) the COTH-d method, (c) the COTH-m method, and (d) the COTH method

	Reference			
	Crown (m^2)	Non-crown (m^2)	Sum	User's Accuracy
Crown (m^2)	2,344.12	3,628.81	5,972.93	39.25%
Non-crown (m^2)	142.34	501.98	644.32	77.91%
Sum	2,486.46	4,130.79	6,617.25	
Producer's Accuracy	94.28%	12.15%		
Overall Accuracy	43.01%			

(a)

	Reference			
	Crown (m^2)	Non-crown (m^2)	Sum	User's Accuracy
Crown (m^2)	1,927.03	2,026.54	3,953.57	48.74%
Non-crown (m^2)	560.44	2,103.24	2,663.68	78.96%
Sum	2,487.47	4,129.78	6,617.25	
Producer's Accuracy	77.47%	50.93%		
Overall Accuracy	60.91%			

(b)

	Reference			
	Crown (m^2)	Non-crown (m^2)	Sum	User's Accuracy
Crown (m^2)	1,811.17	1,576.96	3,388.13	53.46%
Non-crown (m^2)	675.29	2,553.83	3,229.12	79.09%
Sum	2,486.46	4,130.79	6,617.25	
Producer's Accuracy	72.84%	61.82%		
Overall Accuracy	65.96%			

(c)

	Reference			
	Crown (m^2)	Non-crown (m^2)	Sum	User's Accuracy
Crown (m^2)	1,262.48	594.04	1,856.52	68.00%
Non-crown (m^2)	1,224.99	3,535.74	4,760.73	74.27%
Sum	2,487.47	4,129.78	6,617.25	
Producer's Accuracy	50.75%	85.62%		
Overall Accuracy	72.51%			

(d)

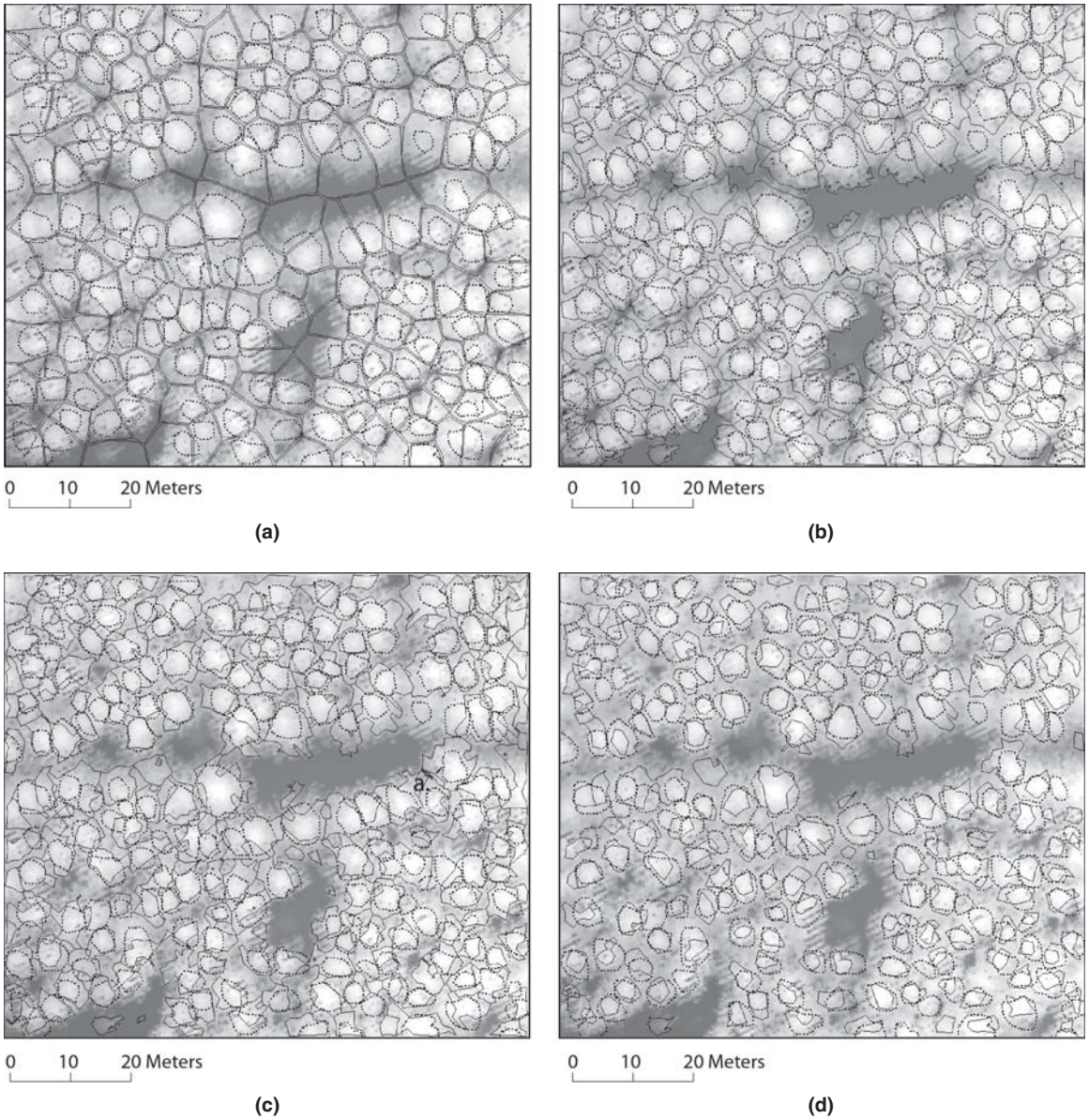

Figure 6. Tree crown delineation using (a) the watershed method, (b) COTH-D, (c) COTH-M, and (d) the COTH method. Reference crowns are dotted lines in all figures.

the reference data, and is a more stringent measure than the visual affirmation used by Kwak *et al*. (2007). The reason for the poor AATI performance likely lies within the study area, dense forest with significant gaps.

Four crown-based metrics for the reference crowns and those delineated from the four methods are summarized in box plots in Figure 8. The watershed method overestimated the area and perimeter of tree crowns. The COTH-D and COTH-M methods delineated crowns with a range of shape and size, resulting in larger value ranges of the metrics. The metrics for the crowns delineated using the COTH method show the most similar patterns to those for the reference crowns (Figure 8). Four landscape-based metrics for the study area are also summarized in Table 6. The watershed method resulted in very large values of the landscape-based metrics, which means that it was not effective to identify non-tree area (i.e., canopy gaps). The landscape-based metrics for the results of the COTH and COTH-M methods were relatively close to those for the reference map.

Discussion

A major cause of the difference in accuracy between watershed segmentation and the COTH method lies within those crowns that are not correctly segmented. Both methods may have failed to identify a tree crown correctly, yet the magnitude of the error for such crowns in a watershed segmentation method is much more pronounced than in the COTH method. In forest conditions such as the ones used in this study, where trees are densely populated yet large canopy gaps exist, watershed processing will produce large canopies for those trees bordering the gaps. Such extended crowns can be trimmed by applying a height threshold, but no such threshold readily. In addition, no height threshold

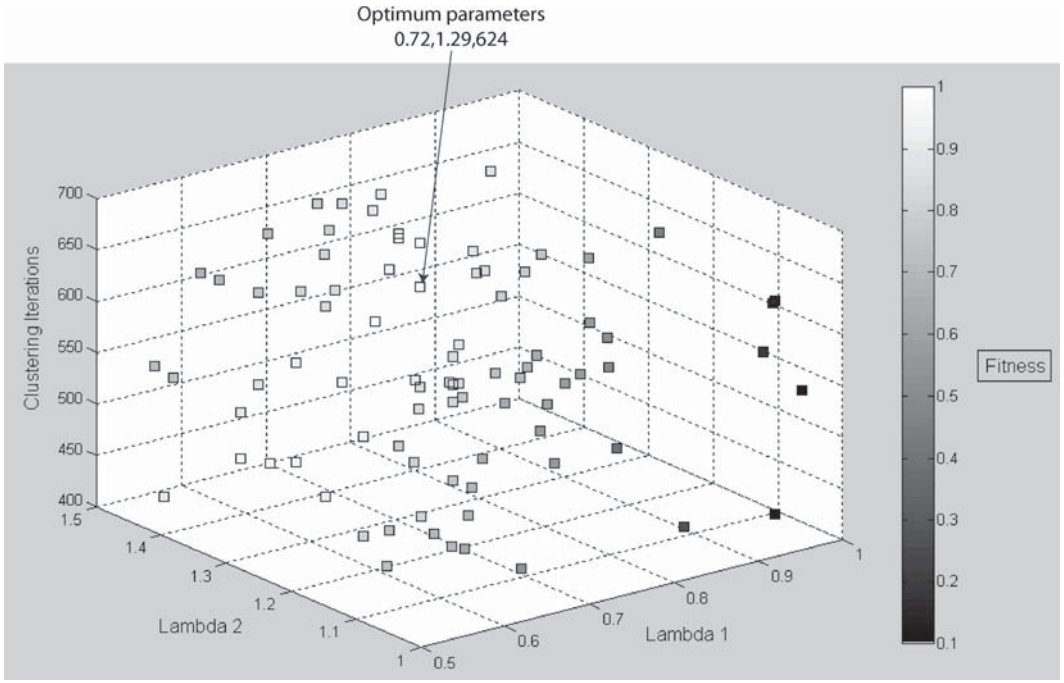

Figure 7. GA optimization results. The three axes correspond to λ_1, λ_2, and the number of iterations used for each execution of the clustering algorithm. The color of the symbols corresponds to the fitness of that particular combination of parameters, and the optimum fitness is shown.

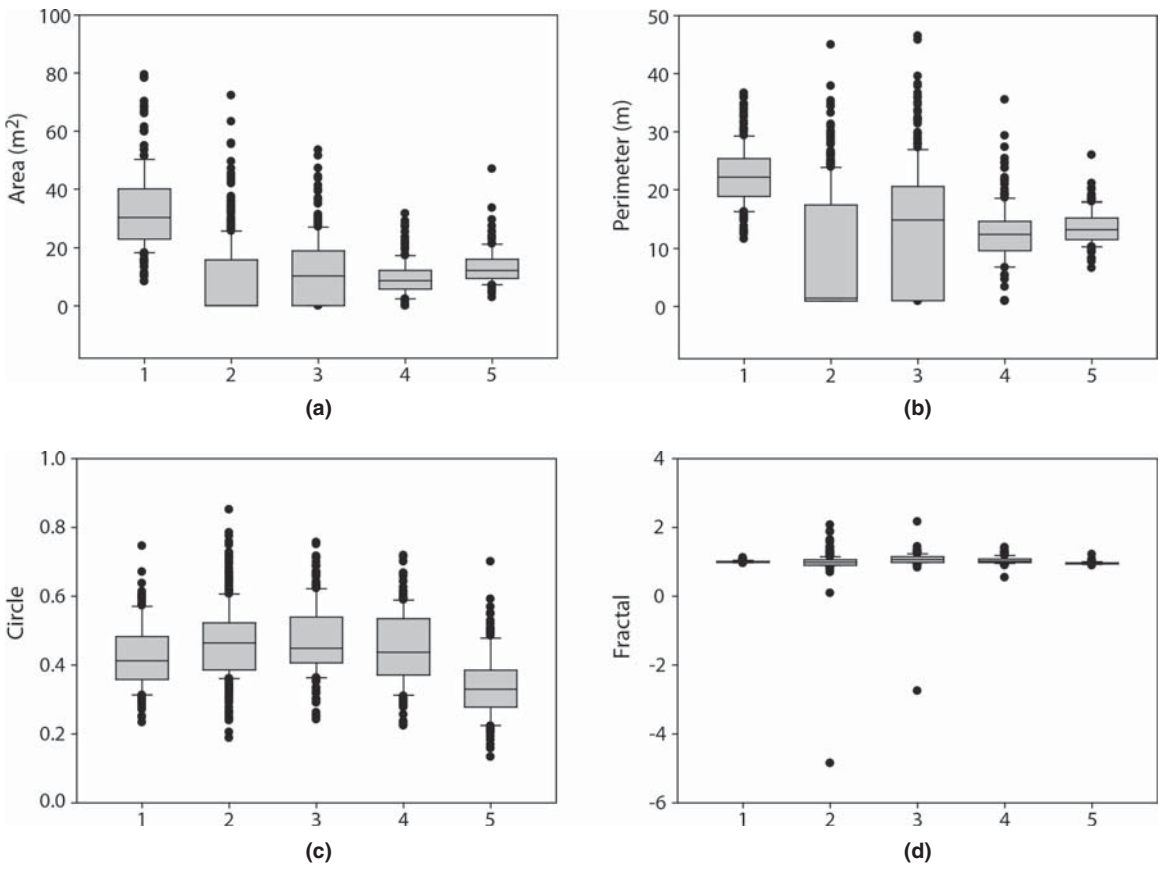

Figure 8. Box plots of the four crown-based metrics: (a) area, (b) perimeter, (c) circle, and (d) fractal. The *x* axis represents the four methods (1: watershed; 2: COTH-D; 3: COTH-M; 4: COTH); and (5) the reference in all plots. The 25th and 75th percentiles were applied for the box, and the 10th and 90th percentiles for the whiskers.

TABLE 6. LANDSCAPE-BASED METRICS CALCULATED FOR REFERENCE CROWNS AND THOSE PRODUCED BY DELINEATION METHODS

Method	Contagion	Division	Split	Perimeter-Area Fractal
Watershed	67.2	0.985	66.053	2.176
COTH-d	41.8	0.815	5.410	1.194
COTH-m	40.3	0.683	3.159	1.239
COTH	49.7	0.482	1.930	1.155
Reference	44.4	0.608	2.553	1.114

TABLE 7. SUMMARY OF CONFUSION MATRICES OF TREE CROWN DELINEATION RESULTS FOR ADDITIONAL PLOTS (FROM GLEASON AND IM, 2011B)

Plot	Overall	User's accuracy		Producer's accuracy	
		crown	non- crown	crown	non- crown
1*	66.1%	53.2%	74.7%	58.2%	70.7%
2*	63.6%	57.7%	67.6%	54.2%	70.6%
3	66.7%	59.1%	71.8%	58.4%	72.4%
4*	63.7%	42.5%	78.0%	56.5%	66.9%
5	53.3%	43.0%	60.2%	41.7%	61.4%
6*	70.8%	69.2%	71.8%	62.0%	77.8%
7	69.1%	50.0%	81.4%	63.6%	71.6%
8*	62.9%	65.9%	61.0%	52.6%	73.1%
9	69.5%	59.7%	76.1%	62.5%	73.9%
10*	53.3%	40.3%	62.7%	43.6%	59.4%
11*	61.4%	42.5%	73.9%	51.8%	66.1%
12*	71.5%	75.7%	68.7%	61.1%	81.4%
13*	61.3%	52.4%	67.2%	51.7%	67.9%
14	65.4%	57.8%	70.5%	56.9%	71.3%
15	62.3%	58.7%	64.7%	52.9%	69.9%
16	57.4%	54.1%	59.5%	47.2%	66.0%
17	56.4%	52.7%	58.9%	45.6%	65.6%
18*	69.2%	61.1%	74.4%	60.4%	75.0%

* Symbol Refers to a Hardwood-Dominant Plot

readily presents itself to distinguish between which of these crown areas do and which do not belong to trees, as lidar data collected over dense forest will account for smaller vegetation beginning to grow in such gaps. This then represents a major weakness of watershed segmentation for tree crown delineation, as the method is unable to distinguish between canopy and non-canopy.

In order to discuss the transferability of the COTH method, we used the results from Gleason and Im (2011b), where the COTH method was applied to ten mixed deciduous and eight conifer stands located in Heiberg Memorial Forest for biomass quantification. Targeting 40 percent of the plot area as the GA fitness goal, the COTH method was applied to each plot and the results are displayed in Table 7. Figure 9 gives two examples of the COTH method as applied to different forest stands that are more heterogeneous than the original study plot. The 40 percent plot area assumption was derived from comparing the total crown area for each plot versus the total plot footprint for that area, and is reasonable for most of these plots. These additional plots were structurally heterogeneous, representing forest stands of different ages and management techniques, and most also contain similar gaps and problem areas as the original study plot. Overall accuracies range from 53.3 percent to 71.5 percent, with mean delineation accuracy 64.4 percent for hardwoods and 62.5 percent for softwoods (Table 7). Delineation accuracies are lower than the accuracy of the plot for which the method was developed because a standard crown area

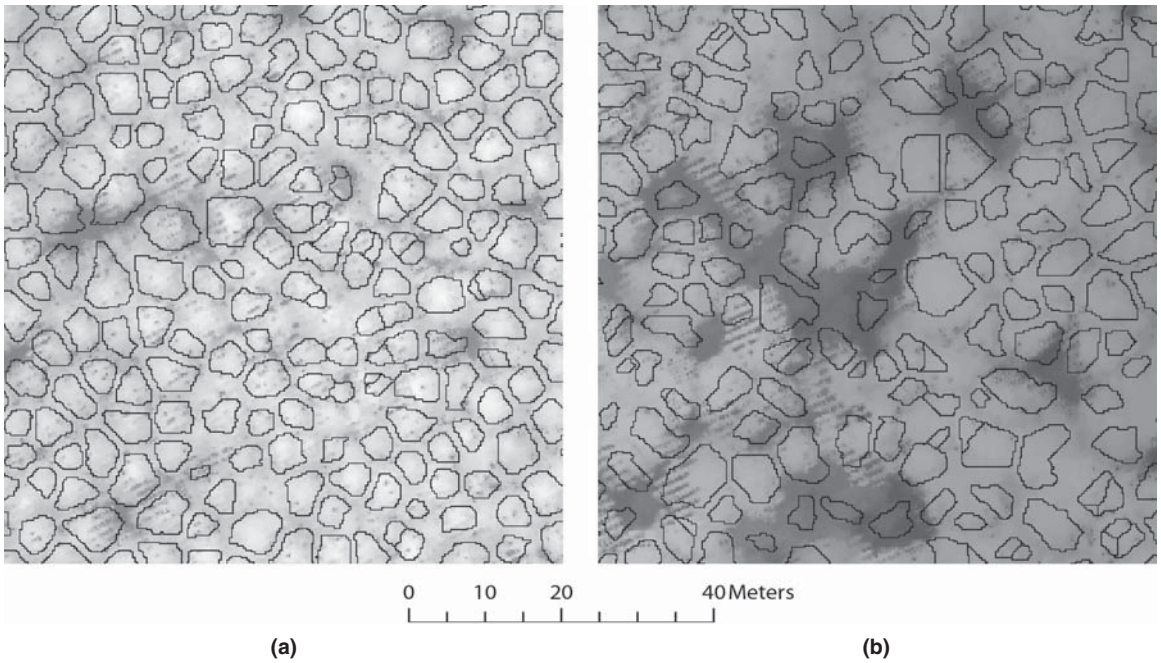

Figure 9. Two other crown delineation examples: (a) a softwood (*Picea abies*)-dominant plot (#7), and (b) a hardwood-dominant plot (#6). The hardwood-dominant plot contains several different hardwood species found in the northeastern US including *Acer saccharum, Fagus grandifolia,* and *Betula papyrifera*. Data for these plots were obtained from Gleason and Im (2011b). Refer to Table 7 for the accuracy associated with the plots.

assumption was used for each plot to test the transferability of the method. As previously discussed, there are several methods for assessing delineation accuracy, and these results demonstrate the chosen representation of accuracy for this study. When removing non-crown measures of accuracy, the overall crown accuracy (user's and producer's) falls to 54.9 percent for the 18 additional study plots, respectively. However, it is important to include non-crown measures of accuracy in tree crown delineation in moderate dense forests to assure that major gaps within a forest are not included as extensions of correctly identified treetops. An alternative approach to managing such gaps might be to apply a height threshold, thus assuming that all areas below a certain height are automatically excluded from the delineation. Such an assumption might preclude those trees that grow on the border of a forested stand or are regenerating within canopy gaps within a mature forest. By not eliminating any forested area and including non-crown area for accuracy assessment, this accuracy assessment will emphasize the ability of the method to place tree crowns within the canopy and not within any gaps that may be present. The detailed descriptions associated with the stands and tree crown delineation results are found in Gleason and Im (2011b).

In the object recognition procedure, of interest is the spatial cluster of higher fitness values that correspond to the optimum range of parameters. In Figure 7, there is a *vein* of results that correspond to the ratios of λ_1 and λ_2 that yield the most accurate results and occur in ratios between 1.2 and 1.5 λ_1 / λ_2. Also, more iterations seem to generally increase the fitness of the results, but it appears that the ratio of λ_1 / λ_2 is the major driver behind the clustering process. Fitness is reported as the percent similarity between the reference crown area and the area produced by the clustering. While some of these fitness values are quite high, the high fitness does not mean that the accuracy of the delineation is equally robust. The hill climbing process decreases the total crown area and removes the potential for a perfect solution, but the process is necessary to remove extra crown objects and to separate those clusters containing more than one crown. Two parameters, μ and υ, were constrained in the final GA to equal 1, the default value. This decision was made after it was found that these parameters had negligible impacts on the solution when watershed lines, rather than the default setting of an image border, were used as initial contours.

It is likely that other object recognition methods such as image segmentation-based approaches (e.g., those built in *e*Cognition software) would perform similarly to the method of Li *et al.* (2007) used in the COTH method, yet each object recognition method still requires an input set of parameters. The parameters needed to identify crown objects will change according to lidar point density and differences in site conditions and tree species, and using default values or manually setting these parameters for different sites may not yield optimum performance. Applying a GA can efficiently optimize these parameters and improve the final delineated accuracy, which requires no additional data or knowledge of the study site. The fitness function used to direct the GA is paramount to finding a robust solution, and in this study the total area of reference crowns was used to test the accuracy of each chromosome. The number of treetops identified using maxima filtering and contained within a crown object was considered as a component of fitness, but was not included in the final GA for two reasons. First, it was difficult to discern a practical weighting to assign to the areal and treetop measures of fitness, as the area of the crowns compared to the reference crowns was deemed the most important outcome of the object recognition step. Second, using the watershed lines as initial contours guaranteed that each treetop identified would be included in the beginning iterations of the object recognition. This introduces a propagation of error if the treetop detection is poor, and including a treetop count measure of fitness would artificially inflate it and lead to less accurate results.

It is possible that both watershed segmentation and the COTH method produced better results than the human interpreters at finding the tree crowns. When manually delineating imagery, there is often a clear separation of tree crowns at the top of the canopy, yet in valleys between dominant crowns it is difficult to determine which areas belong to which crown. In addition, there may be many subdominant (i.e., understory) trees that artificially "fill out" some canopies or that are completely shadowed by dominant crowns. The result is a crown map in which the boundaries of reference crowns are clearly separated, yet in most stand conditions the boundaries of tree crowns will overlap. Watershed processing does a better job of mimicking this facet of dense stands, but will vastly overestimate crown area in gaps and at the edges of such plots. The COTH method tended to over segment tree crowns, which is most likely due to the smoothness of the lidar surface. In optical imagery, shadowing creates clearly defined crowns, whereas the active lidar sensor will not have such shadowing (Figure 2). This smooth surface is more difficult to segment using object recognition, which explains why accuracies of studies using imagery for crown delineation are generally higher than those using lidar data. Yet, as airborne lidar remains a premier sensor for biomass estimation (Gleason and Im, 2011a), the ability to delineate individual trees without ancillary data reduces data collection costs and preprocessing time.

Changing the statistical confidence level of the treetop location process to obtain different widths of the prediction confidence interval had little effect on the number of treetops correctly identified, yet no other means of determining the size of the search window is readily apparent. The delineation of reference tree crowns was conducted in accordance with previous research and provides a reasonable representation of the field conditions, yet any crown delineation made manually from imagery contains inherent human error.

There is a noticeable lack of standardization of how to compute the accuracy of crown delineation studies, as evidenced through the literature review on the topic. The area-based confusion matrix, one of the accuracy metrics that we used, is reasonable for a moderately dense to dense forest where crown area covers approximately more than 35 percent of the study area under investigation. However, using confusion matrices to assess tree crown delineation would not be a good choice for a sparse forest as non-crown area could significantly inflate accuracy. Using the averaged crown area (about 40 percent of the plot area) as the fitness function in the COTH model in this study resulted in relatively low producer's accuracy of crown (51 percent) but high overall accuracy (73 percent). By increasing the fitness function value (e.g., 50 percent or 60 percent) in the COTH model, the higher producer's accuracy of crown could be achieved, but overall accuracy did not increase when tested. However, such a fitness function allows much greater flexibility to the COTH method, and also allows adaptation to differing forest conditions. The COTH method can be further improved by incorporating crown shape or crown location along with crown area into the fitness function. While the COTH method was evaluated over the moderately dense forest plots with various tree species, it should be further investigated for different forest environments such as savannah or tropical dense forests.

Conclusions

The goal of this study was to detect and delineate tree crowns with an automated method, which was largely successful. While the COTH method is completely automated, it is not entirely transferrable. In the treetop detection step, field data is needed to determine the relationship between tree height and crown width, and therefore determining the size of the search window for local maxima is not a fully transferrable process, as it is dependent on site specific regression. However, the success achieved by extending the COTH delineation to additional forested plots of differing ages and species provides evidence that the method is an effective means of tree crown delineation for more forest types than those for which the method was first conceived and tested. It can also be assumed that COTH delineation would be extremely effective in a sparse forest or other environment with few trees or large gaps (e.g., parks, orchard, street trees). The COTH method is independent, however; and five parameters were optimized heuristically, removing a level of user dependence. There are also very few static thresholds in the method, making this study a step towards transferrable estimates of biomass that can be applied across a variety of forest types.

Further research will investigate whether this treetop delineation is suitable for biomass estimation from lidar data and whether biomass estimation transferrable for a range of forest types is feasible. Also in future, using the GA to assign dynamic parameter values to the object recognition may yield even more accurate and efficient results by assessing fitness after a certain number of iterations of the object recognition method. While the accuracy of the final GA derived result is good, there are some final crown objects that are not shaped as one would expect a natural crown to appear from a nadir view. This is likely a product of the number of iterations used to find each crown object, and could be amended by allowing for longer processing time with increased iterations, or by applying shape based morphology to the final product. These concepts were not applied in this research, as changing the shape of the final crown objects would require expert knowledge, thus reducing the automation of the process and potentially making the hill climbing step redundant. Following these results, it may be said that the COTH method provides a significant improvement in classification accuracy for tree crown delineation in similar forest conditions.

References

Bortolot, Z.J., and R.H. Wynne, 2005. Estimating forest biomass using small footprint lidar data: An individual tree-based approach that incorporates training data, *ISPRS Journal of Photogrammetry and Remote Sensing*, 59(6):342–360

Brandtberg, T., 2007. Classifying individual tree species under leaf-off and leaf-on conditions using airborne lidar, *ISPRS Journal of Photogrammetry and Remote Sensing*, 61(5):325–340.

Breidenbach, J., E. Næsset, V. Lien, T. Gobakken, and S. Solberg, 2010. Prediction of species specific forest inventory attributes using a nonparametric semi-individual tree crown approach based on fused airborne laser scanning and multispectral data, *Remote Sensing of Environment*, 114(4):911–924.

Bunting, P., and R. Lucas, 2006. The delineation of tree crowns in Australian mixed species forests using hyperspectral compact airborne spectrographic imager (CASI) data, *Remote Sensing of Environment*, 101(2):230–248.

Castilla, G., G.J. Hay, and J.R. Ruiz-Gallardo, 2008. Size-constrained region merging (SCRM): An automated delineation tool for assisted photointerpretation, *Photogrammetric Engineering & Remote Sensing*, 74(4):409–419.

Chan, T., and L. Vese, 2001. Active contours without edges, *IEEE Transactions on Image Processing*, 10:266–277.

Chang, D., X. Zhang, and C. Zheng, 2009. A genetic algorithm with gene rearrangement for k-means clustering, *Pattern Recognition*, 42(7):1210–1222.

Chen, G., G.J. Hay, and Y. Zhou, 2010. Estimation of forest height, biomass and volume using support vector regression and segmentation from LiDAR transects and QuickBird imagery, *Proceedings of the 2010 18th International Conference on Geoinformatics*, 18-20 June, Beijing, China.

Chen, Q., D. Baldocchi, P. Gong, and M. Kelly, 2006. Isolating individual trees in a savanna woodland using small footprint LiDAR data, *Photogrammetric Engineering & Remote Sensing*, 72(8):923–932.

Chen, Q., P. Gong, D. Baldocchi, and Y.Q. Tian, 2007. Estimating basal area and stem volume for individual trees from LiDAR data, *Photogrammetric Engineering & Remote Sensing*, 73(12):1355–1365.

Coops, N.C., M.A. Wulder, D.S. Culvenor, and B. St-Onge, 2004. Comparison of forest attributes extracted from fine spatial resolution multispectral and LiDAR data, *Canadian Journal of Remote Sensing*, 30(6):855–866.

Fang, H., S. Liang, and A. Kuusk, 2003. Retrieving leaf area index using a genetic algorithm with a canopy radiative transfer model, *Remote Sensing of Environment*, 85(3):257–270.

Gleason, C.J., and J. Im, 2011a. A review of remote sensing of forest biomass and biofuel: Options for small scale applications, *GIScience and Remote Sensing*, 48(2):141–170.

Gleason, C.J., and J. Im, 2011b. Forest biomass estimation from airborne LiDAR data using machine learning approaches, *Remote Sensing of Environment*, in revision.

Goldberg, D.E., 1989. *Genetic Algorithm in Search, Optimization, and Machine Learning*, Addison-Wesley, Boston, Massachusetts.

Gong, B., J. Im, and G. Mountrakis, 2011. An artificial immune network approach to multi-sensor land use/land cover classification, *Remote Sensing of Environment*, 115(2):600–614.

Gonzalez, P., G.P. Asner, J.J. Battles, M.A. Lefsky, K.M. Waring, and M. Palace, 2010. Forest carbon densities and uncertainties from LiDAR, QuickBird, and field measurements in California, *Remote Sensing of Environment*, 114(7):1561–1575.

Gougeon, F.A., 1995. A crown-following approach to the automatic delineation of individual tree crowns in high spatial resolution aerial images, *Canadian Journal of Remote Sensing*, 21(3):274–284.

Im, J., Z. Lu, and J.R. Jensen, 2011. A genetic algorithm approach to moving threshold optimization for binary change detection, *Photogrammetric Engineering & Remote Sensing*, 77(2):167–180.

Jang, J., V. Payan, A.A. Viau, and A. Devost, 2008. The use of airborne LiDAR for orchard tree inventory, *International Journal of Remote Sensing*, 29(6):1767–1780.

Kato, A., L.M. Moskal, P. Schiess, M.E. Swanson, D. Calhoun, and W. Stuetzle, 2009. Capturing tree crown formation through implicit surface reconstruction using airborne LiDAR data, *Remote Sensing of Environment*, 113(6):1148–1162.

Ke, Y., W. Zhang, and L.J. Quackenbush, 2010. Active contour and hill climbing for tree crown detection and delineation, *Photogrammetric Engineering & Remote Sensing*, 76(10):1169–1181.

Koch B., 2010. Status and future of laser scanning, synthetic aperture radar and hyperspectral remote sensing data for forest biomass assessment, *ISPRS Journal of Photogrammetry and Remote Sensing*, 65(6):581–590.

Kwak, D., W. Lee, H. Cho, S. Lee, Y. Son, M. Kafatos, and S. Kim, 2010. Estimating stem volume and biomass of *Pinus koraiensis* using LiDAR data, *Journal of Plant Research*, 123(4):421–432.

Kwak, D., W. Lee, J. Lee, G.S. Biging, and P. Gong, 2007. Detection of individual trees and estimation of tree height using LiDAR data, *Journal of Forest Research*, 12(6):425–434.

Li, C., C.Y. Kao, J.C. Gore, and Z. Ding, 2007. Implicit active contours driven by local binary fitting energy, *Proceedings of the 2007 IEEE Conference on Computer Vision and Pattern Recognition,* 17-22 June, Minneapolis, Minnesota, pp. 1–7.

Lin, C., G. Thomson, C. Lo, and M. Yang, 2011. A multi-level morphological active contour algorithm for delineating tree crowns in mountainous forest, *Photogrammetric Engineering & Remote Sensing*, 77(3):241–249.

Næsset, E., and T. Økland, 2002. Estimating tree height and tree crown properties using airborne scanning laser in a boreal nature reserve, *Remote Sensing of Environment*, 79(1):105-115.

Persson, Å., J. Holmgren, and U. Söderman, 2002. Detecting and measuring individual trees using an airborne laser scanner, *Photogrammetric Engineering & Remote Sensing*, 68(9): 925–932.

Popescu, S.C., 2007. Estimating biomass of individual pine trees using airborne LiDAR, *Biomass and Bioenergy*, 31(9):646–655.

Popescu, S.C., and R.H. Wynne, 2004. Seeing the trees in the forest: Using LiDAR and multispectral data fusion with local filtering and variable window size for estimating tree height, *Photogrammetric Engineering & Remote Sensing*, 70(5):589–604.

Popescu, S.C., R.H. Wynne, and R.E. Nelson, 2002. Estimating plot-level tree heights with LiDAR: Local filtering with a canopy-height based variable window, *Computers and Electronics in Agriculture*, 37(1-3):71–95.

Rezende, M.C.A.F., C.B.B. Costa, A.C. Costa, M.R.W. Maciel, and R.M. Filho, 2008. Optimization of a large scale industrial reactor by genetic algorithms, *Chemical Engineering Science*, 63(2):330–341.

Tseng, M., S. Chen, G. Hwang, and M. Shen, 2008. A genetic algorithm rule-based approach for land-cover classification, *ISPRS Journal of Photogrammetry and Remote Sensing*, 63(2):202–212.

Van Aardt, J.A.N., R.H. Wynne, and J.A. Scrivani, 2008. LiDAR-based mapping of forest volume and biomass by taxonomic group using structurally homogenous segments, *Photogrammetric Engineering & Remote Sensing*, 74(8):1033–1044.

Vauhkonen, J., I. Korpela, M. Maltamo, and T. Tokola, 2010. Imputation of single-tree attributes using airborne laser scanning-based height, intensity, and alpha shape metrics, *Remote Sensing of Environment*, 114(6):1263–1276.

Wang, L., P. Gong, and G.S. Biging, 2004. Individual tree-crown delineation and treetop detection in high-spatial-resolution aerial imagery, *Photogrammetric Engineering & Remote Sensing*, 70(3):351–357.

Wang, Y., 2005. A GA-based methodology to determine an optimal curriculum for schools, *Expert Systems with Applications*, 28(1):163–174.

Wulder, M., K.O. Niemann, and D.G. Goodenough, 2000. Local maximum filtering for the extraction of tree locations and basal area from high spatial resolution imagery, *Remote Sensing of Environment*, 73(1):103–114.

Zhao, K., S. Popescu, and R. Nelson, 2009. LiDAR remote sensing of forest biomass: A scale-invariant estimation approach using airborne lasers, *Remote Sensing of Environment*, 113(1):182–196.

(Received 18 March 2011; accepted 02 August 2011; final version 22 November 2011)